Cyclic Loading of Dental Implants in a Controlled Environment

Summary of dissertation for the degree of Master in Bioengineering and Nanosystems

Margarida Janardo[1]
[1]Instituto Superior Técnico, University of Lisbon, Portugal
margarida.janardo@tecnico.ulisboa.pt

ABSTRACT

One of the existing ways to restore the aesthetic and/or masticatory function of an individual who has lost teeth are dental implants. The stability of these devices within the oral environment may be affected by several factors, such as human saliva, repeated masticatory forces and implant characteristics. The objective of this study was to evaluate the effect of an electrolytic solution of artificial saliva, without fluoride, on the stability of dental implant systems with different surface finishes (sandblasted and sandblasted+acid etching) and implant-abutment geometries (external hexagonal and Morse taper). The samples were analysed using mechanical fatigue tests and nanotribological tests, both in aqueous medium, among other technics. In the first test, the connection that showed the greatest displacement was MT with HSA. In the second test, the friction coefficients indicated the lubricant is capable of penetrate between the implant-abutment interface, and the wear of the samples appeared to be derived from abrasion and adhesion of the tribological pair CP Ti grade 4/Ti_4Al_6V. It was possible artificial saliva contributed to increase the wear of the samples, triggering a corrosive action on the metallic implants.

Keywords

Dental implants; Artificial saliva; Fatigue tests; Nanotribological tests; Scanning electron microscopy; X-ray computed microtomography.

1. INTRODUCTION

One of the existing ways to restore the aesthetic and/or masticatory function of an individual who has lost teeth are dental implants [1]. A dental implant system is composed of four parts: the implant, which replaces the natural root of the teeth; the crown, which represents the natural crown; the abutment, which promotes implant-crown attachment; and the screw, which makes the implant-abutment joint [2]. Within the oral cavity, these systems are in contact with human saliva and are subjected to repeated masticatory forces. Although it has organic and inorganic substances that help maintain the integrity of teeth (pH 6.7-7.4) [3, 4], saliva does not seem to have the same protective effect on the material of dental implants[5]. Although it helps to chew food, masticatory forces may weaken the stability of the implants in alveolar bone in long term [6], which may also be influenced by other factors, like implant-abutment connection and surface treatment of the implant [7–11]. According to Feitosa *et al*, Morse taper (MT) geometry is more stable than external hexagonal (HE) configuration in cyclic fatigue tests [12, 13]. The results presented by Elias *et al* revealed that implants treated with sandblasted + acid etching (TiO_2 particles + HNO_3 or HF) had a mean roughness value (R_a between 1.0-2.0 μm) higher than those treated only with acid (H_2SO_4 and HCl) or machining (0.3-1.0 μm) [14, 15]. Although they have proven advantages, the sandblasting and acid etching surfaces may present microcracks related to acid corrosion, which may decrease fatigue strength and increase the likelihood of mechanical fracture [16].

Although Implantology has evolved considerably, dental implant systems continue to present problems in both the implant-abutment connection and bone-implant interface. One way to predict the long-term stability of these systems is to resort to mechanical fatigue testing of dental implants. In this way, it is possible to know how saliva (artificial fluid) and an individual's masticatory cycles (repetitive cyclic loads) [12, 17, 18] interfere with osseointegration and/or contribute for the deformation or fracture of the system [17]. Shemtova-Yona *et al* performed fatigue tests on Ti_6Al_4V implants in a dry environment and in artificial saliva containing 250 ppm of sodium fluoride and found that environmental conditions similar to those found in the oral cavity can accelerate

implant fatigue [18]. Later, the same authors reinforce that the corrosion of titanium is not a cause for failure by implant fatigue, but rather a mechanism that promotes the propagation of cracks caused by cyclic loads [19].

Although metallic or alloy implants have a high success rate, their failures have been caused mostly (about 90%) by fatigue wear, which decreases the load resistance gradually [17, 20]. In part, the corrosion wear resulting from leaching of the metal ions due to food acids has also been mentioned as a possible cause of failure of these implants. One of the most used methods to study the tribological behavior of the dental materials is the in vitro simulation in the laboratory, being possible to represent the in vivo conditions (masticatory cycle and human/artificial saliva). As a rule, titanium alloys have better tribological properties and resistance to abrasion and plastic deformation than commercially pure titanium (CP Ti), but lower corrosion resistance [16, 20, 21].

In turn, saliva has been described as a potentiator of a simultaneously corrosive and erosive effect. For the latter case, tribocorrosion arose, which is defined as the "degradation of tribological contact that results from the combined effect of metal removal by mechanical wear and electrochemical oxidation". The implant-screw interfaces may suffer from this mechanical and chemical phenomenon [22], since they are exposed to cyclic masticatory loads and salivary fluid, whose solvent is able to penetrate a few micrometers deep and change the friction coefficient and wear.

1.1 Objectives

The objective of this study was to evaluate the effect of an electrolytic solution of artificial saliva, without fluoride, on the stability of dental implant systems with different surface finishes (sandblasted and sandblasted+acid etching) and implant-abutment geometries (EH and MT). These grade 4 CP Ti implants were inserted into polyurethane foam and epoxy composite to mimic the denser trabecular bone and cortical bone, respectively. The displacement of the specimens was analysed by mechanical fatigue tests in aqueous medium, and their deformations were verified by scanning electron microscopy (SEM) and computed microtomography (micro-CT). Additionally, the surface composition of the samples, subject and not subject to the fatigue tests, was determined by energy-dispersive X-ray spectroscopy (EDS). The friction coefficient of the tribological pair CP Ti/Ti_6Al_4V, whose samples were submitted or not to the fatigue tests, was calculated through the nanotribological tests in artificial saliva. The wear of the implants and abutments was observed by SEM.

2. MATERIALS AND METHODS

2.1. Characterization of rigid polyurethane foam and epoxy composite

Both rigid polyurethane (PU) foam and short fiber epoxy composite have homogeneous characteristics that eliminate the heterogeneity and anisotropy of the trabecular and cortical bone, respectively. Thus, this foam with 95 % of closed cells can be used as a "bone model" to support implants in compression tests, according to the standard ASTM F1839-08 [R16] [23–26]. From Sawbones (Vashon Island, Washington, USA), the PU foam with the highest density (reference #1522-12) and the epoxy composite with a thickness of 2 mm (reference #3401-01) were obtained.

2.2. Characterization of dental implants and their abutments

The dental implant systems (DIO• Implant®) involved the following implant-abutment connections and surface treatments: (1) external hexagonal (EH) treated with resorbable blast media (RBM); (2) Morse taper (MT) treated with hybrid sandblasted acid etched (HSA); and (3) MT treated with RBM [16]. The RBM treatment consists on the high pressure projection of hard biocompatible hydroxyapatite microparticles [27–31]; the HSA treatment consists on the projection of TiO_2 particles and, later, the use of 10 % HCl:10 % H_2SO_4 (1:1 V/V) to dissolve the embedded particles [32, 33]. The material of the components of the dental systems was

commercially pure titanium (CP Ti) grade 4, and their purity is essentially characterized by a maximum medium weight of 0.5 % of iron, 0.4 % of oxygen, and 0.1 % of carbon [16, 34, 35].

2.3. Preparation of polyurethane and epoxy samples and artificial saliva

PU cubes (15×15×13.5 mm^3) and epoxy pieces (15×15×2 mm^3) were obtained and then glued to mimic the the set of two substrates present in the bone structure. Each sample was drilled using a technique adapted from the surgical protocol, according to the type of implant system. An implant, abutment and screw were placed in each bored sample, using a method also based on the surgical protocol.

The artificial saliva was prepared following a composition elaborated by Göhring *et al*, which included: 1.86 g/L $NaHCO_3$; 1.20 g/L KCl; 0.85 g/L NaCl; 0.35 g/L KH_2PO_4; 0.0495 g/L H_3BO_3; 0.10 g/L $CaCl_2 \cdot 2H_2O$; 0.0389 g/L KSCN e 0.0407 g/L $MgCl_2 \cdot 6H_2O$ [36]. The pH value of this saliva was adjusted to 7.0 (at 25 °C).

2.4. Standard ISO 14801:2007 for fatigue testing of dental implants

The mechanical fatigue tests were adapted from the standard ISO 14801:2007, Dynamic Fatigue Test for Endosseous Dental Implants [37]. The implants were positioned at a distance of 3.0 mm ± 0.1 mm from the artificial bone surface, to represent the worst-case scenario for marginal bone resorption, which may occur in vivo after implantation. A hemispherical piece was placed at the free end of the abutment, capable of replacing the crown. The specimen support formed an angle of 30° ± 1° between the loading and implant axis, thus reproducing the loading of a dental implant into the oral cavity [38]. The tests were performed in saline solution, and the mean force, mean frequency and number of cycles applied were -75 N, 6 Hz and 1.2×10^5, respectively. In this work, Bicudo's protocol was followed, in which the implant is inserted in an artificial support that simulates the natural bone [39].

2.5. Computerized microtomography (micro-CT)

A computed microtomograph SkyScan 1172 from Bruker (Kontich, Belgium), containing a Hamamatsu Photonics microfocus X-ray source and controlled by the SkyScan® software, was used to study the foam and implant of each type of connection/treatment, after being submitted to the mechanical tests. In terms of the procedure, the micro-CT was based on the following steps: (1) acquisition of 2D radiographic images; (2) 3D reconstruction of the object; and (3) analysis of the 3D image obtained. In the first step, variables like the X-ray source voltage and current, type of filter, and voxel size (18.10 μm) were previously chosen for each connection/treatment. Each projection image was acquired with an object rotation pitch of 0.7°, over an angular range of 180°. About 1000 cross-sectional images were generated per sample during the scanning. In the second step, the NRecon® software allowed to choose the volume of interest (VOI), reduce the ring artifacts and correct the beam hardening of each sample. Each projection image was reconstructed on a tomographic cross-section (along the ZZ axis) through the Feldkamp-Davis-Kress (FDK) conic beam algorithm [40, 41]. The tomographic images corresponding to each sample were used to form a 3D solid using the CTvox® software. In the last step, the CTAn® software allowed the binarization of images and the use of a polygon to form the region of interest (ROI) of the slices. After the interpolation of all the ROIs of the VOI, it was possible to quantify the microstructural parameters of the 3D volume.

2.6. Preparation of samples for tribological tests

Prior to the nanotribological tests, the implants/abutments were prepared using a mixture of liquid epoxy resin and a resin hardener, which solidified after 12 h at room temperature. The samples were then polished using a silicon carbide (SiC) sandpaper.

2.7. Nanotribology

A nanotribometer, connected to the InstrumX software, was used to study the rolling model constituted by the polished implant or abutment sample (Ti CP grade 4, body) and precision sphere (Ti_6Al_4V, counter body, radius of 1.5 mm), in a wet environmental (artificial saliva). Each sphere was used three times by the same sample. The nanotribological tests were performed at room temperature, defining: (1) a maximum linear velocity of the sample of 0.65 cm/s, which attempts to simulate the sliding velocity of the teeth during chewing; (2) an half-amplitude of the reciprocal movement of the sample of 0.5 mm – the total amplitude of 1 mm resembles the sliding distance between two teeth; (3) a normal charge (F_N) of 37.53 mN corresponding to an average masticatory force of 316 N; and (4) a number of cycles of 1300, representing approximately the number of masticatory cycles performed by an individual in a day. Given a acquisition frequency of 2.07 Hz, close to the masticatory frequency, each trial had a duration of approximately 10 minutes, which was intended to translate the total time spent chewing over a day. To calculate the F_N to be applied, the masticatory force was considered between 70 and 700 N [42] and the contact area between two teeth was considered to be 2 mm^2. An intermediate loading cantilever (ML-237) was selected. For each test, it was possible to calculate the friction coefficient (μ) of the materials in relative motion under in vitro conditions. The sample-contact area was 238 μm^2.

2.8. Scanning electron microscopy (SEM) and energy dispersive X-ray spectroscopy (EDS)

In the present work, a field emission gun-scanning electron microscope (FEG-SEM) was used to visualize the topography/texture and orientation of the structure of the materials. It has secondary electrons (SEs) and backscattered electrons (BSEs) detectors and has coupled an energy-dispersive X-ray spectroscopy (EDS) system. It allows the acquisition of images with 1.2 nm of spatial resolution. The voltage and vacuum pressure in the test chamber were 15 kV and ~8×10^{-5} Pa, respectively.

To evaluate the damage caused by the fatigue tests and/or by the tribological tests, topographic images of SEM were collected from the implants and abutments subjected and not subjected to the fatigue tests and from the foams submitted to them. However, chemical EDS spectra were only obtained from the implants and abutments surface with and without mechanical trials. Both PU foams and implants/abutments after nanotribological tests were previously coated with a conductive film of gold-palladium alloy, to prevent the accumulation of charges on the samples during the scanning.

3. RESULTS AND DISCUSSION

3.1. Fatigue testing for dental implants

The curves displacement vs. number of cycles (n) obtained for the samples EH with RBM, MT with RBM and MT with HSA (figure 3.1) showed a behaviour similar to that of the curve tension (σ) vs. extension (ε) of a rigid PU foam, subjected to uniaxial compression [43, 44]. This happened because the collapse of the material is much more accelerated in the PU than in the epoxy composite and CP Ti of implant systems [25, 44, 45].

All types of systems tested exhibited an elastoplastic pattern consisting of: (1) linear elastic region, characterized by a sudden increase in displacement for a small number of cycles, and caused by the elastic deformation of the cell walls; and (2) region of plastic collapse, caused by the progressive and permanent plastic collapse of the cells, and where the displacement is maintained relatively constant throughout the cycles. The densification region, corresponding to the abrupt increase in displacement for a large number of cycles, and derived from almost total cell collapse, was not reached in any of the samples [46].

For the EH and MT interfaces, both with RBM, the displacement of the curves obtained in artificial saliva was slightly different from the curves acquired by Bicudo in dry environment, using a lower frequency (3 Hz) and a slightly lower average force (70 N) [39]. Still comparing with the results of this author, it could be verified that, in order to obtain the same displacement in a sample of EH with RBM, at a frequency of 4.5 Hz, it is necessary

to resort to larger mean forces (150 N) in a dry environment and smaller (75 N) in a wet environment, i.e., the required F_{mean} in a dry environment is twice the F_{mean} required in salivary environment.
However, artificial saliva did not seem to exert a great effect on the fatigue behaviour of MT with RBM samples. Overall, the curves obtained from tests with different frequencies revealed a distancing pattern approximately proportional to the applied frequency. As reported by Bicudo [39], increasing frequency promotes a greater displacement of the implants within the foam, while increasing F_{mean} promotes deformation intensification.
Comparing results with similar frequencies, it was found that the interface MT with RBM shares the same displacement as other samples with the: (1) same connection and different treatment (MT with HSA); and (2) same treatment and different connection (EH with RBM). However, the connection EH with RBM was not consensual on this respect, since shared and did not share the same level of movement as other samples with the same treatment (MT with RBM), and also showed no similarity to systems with different connection and treatment (MT with HSA). From the connections tested, MT with HSA showed the greatest deformation, but most of the samples did not reveal the ability to accommodate the micromovements of the implant, having a final displacement greater than 0.1 mm [47] in less than 4.8 months of masticatory function [48].

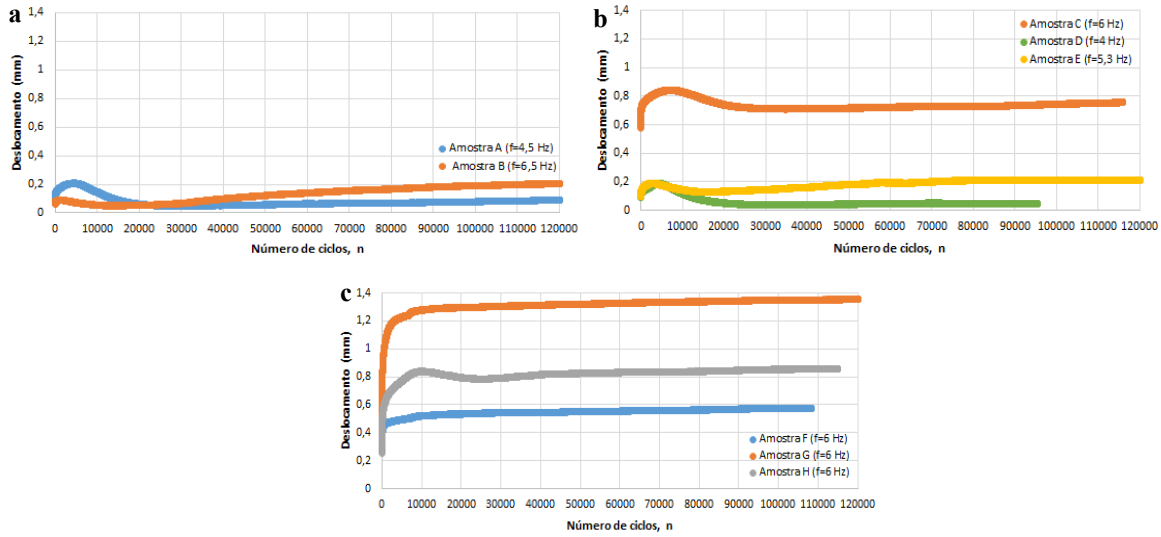

Figure 3.1 – Curves displacement vs. number of cycles obtained for the samples EH with RBM (**a**), MT with RBM (**b**) e MT with HSA (**c**).

3.2. Nanotribology

In nanotribological tests in artificial saliva, the pair Ti CP grade 4/Ti_6Al_4V was used to simulate the contact implant-abutment. For each type of connection/treatment (EH with RBM, MT with RBM and HSA), subjected and not subjected to the fatigue tests, the mean coefficient of friction (μ) of the two materials was calculated. Most of the results remained framed at similar values and less than 0.5, indicating that the lubricant was not completely displaced from the space between the sample and the sphere during relative movement. From these results, it can be seen that saliva is able to penetrate the implant-abutment interface. Only in a few exceptions part of the salivary fluid was displaced from this space, increasing the μ and causing the implant/abutment and sphere asperities to be closer to each other [20]. Comparing the samples with and without cyclic loading, it was verified that the value of the μ of the two materials in artificial saliva was not consistent in both situations. There were samples tested where the coefficients of friction were lower than the respective situations without cyclical load, and vice-versa. Since the difference between both mean coefficients of all the samples subjected and not subject to the fatigue tests was only 0.017, it can be said that the cyclic loads in artificial saliva have little influence on the friction coefficients of the tribological pair Ti CP/Ti_6Al_4V in lubricated environment.

As expected, the mass of all the spheres was smaller after than before the tests, which means the beads transferred matter to the sample/saliva and suffered some wear (mean mass loss of 0.143%). Although the

literature states that the higher μ's lead to higher material losses [49], the results were inconsistent in this regard. Also, although there was no consensus of μ between tested and untested samples, mean mass loss was more significant in implants under cyclic loading (0.275%) than in those not tested (0.090%).

3.3 Micro-CT

Unlike the fatigue tests, the interface that showed the greatest deformation of material in the micro-CT was the MT with RBM, presenting a smaller fraction of the bone volume (BV/TV) and smaller thickness trabecular (Tb.Th). Although the frequency used has an influence on the displacement of the test pieces, it does not seem to have the same effect on the morphometric parameters. Even after the fatigue tests, trabecular separation (Tb.Sp) of samples MT with RBM and with HSA continued within the range defined for foam cell size (0.5 to 1.0 mm), that is, the microstructure of MT samples with RBM and MT with HSA did not undergo major changes with the application of force. However, this result is in agreement with the literature, since the treatment with HSA has shown a better resistance to the fatigue than the finishing with RBM, to allow a better adhesion of the cells [50].

Comparing the shape of the cells, after removal of the implants from the foams, and the shape of the implants, the smaller and larger displacement of the samples EH with RBM and MT with HSA during the cyclic tests was due to the creation of a smaller and larger gap between the implant and the foam, respectively.

3.4 SEM and EDS

According to the SEM, the foam-implant contact surface (delimited to blue) was the most affected region, where it is possible to observe deformation bands (bounded to orange) including several cells (figure 3.2).

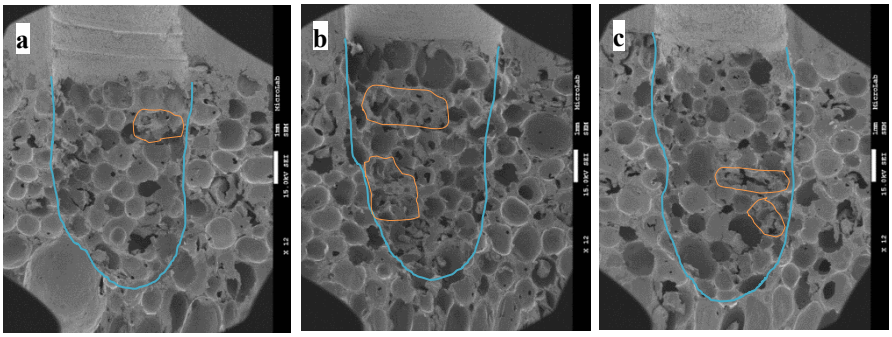

Figure 3.2 – SEM images of the foams belonging to samples EH with RBM (**a**), MT with RBM (**b**) and MT with HSA (**c**), after fatigue tests. Blue line – area affected by the implant. Orange line – deformation bands generated during fatigue tests.

The sample EH with RBM showed the least deformation and the lowest foam-implant area affected, with only one strain band. The sample MT with RBM showed the highest accumulation of damage, exhibiting two bands of deformation with an area superior to that of the bands of the samples EH with RBM and MT with HSA. The sample MT with HSA was the one that showed the largest affected area, denoting two bands of deformation with a lower area than the bands of the sample MT with RBM. All of these results were in agreement with their fatigue curves, because the increase in the affected area and/or the number of collapsed cells in the three samples is related to the increased displacement of the implant. For EH and MT, both with RBM, the Bicudo's images obtained for the same experimental conditions, but in dry environment and frequency of 3 Hz, were different from those obtained in this work in salivary environment and different frequencies, not revealing any collapsed cell. The Bicudo's images more similar to those of this work, with the same frequency, were those acquired for an upper mean force (150 N), having the same number of deformation bands. Once again, it is reinforced the idea that the same level of deformation between the samples EH and MT with RBM can be achieved with a higher average force in dry environment (air) and lower in wet environment (artificial saliva) [39].

By comparing tested and untested implant surfaces in the fatigue, no sharp failure that had been derived from

cyclic salivary loads was found in the samples, as found in the micro-CT. However, it was found that the MT interface fixed the abutments to the implants much better than the EH, which is in agreement with the literature. Unlike the MT bond, the EH connection does not seal enough to prevent the ingress of particles from both artificial saliva and PU foam. The connection that allowed better attachment to the artificial foam was the EH with RBM, which is in conformity with the fatigue tests obtained. However, this result contradicts what is described in the literature, since a HSA surface allows a better integration than a RBM surface [50].

Even comparing the tested and untested samples with artificial saliva, the element mostly detected on the surface of all abutments, without and with fatigue tests, and implants not tested was titanium (Ti), as expected. Although the main element was Ti in the implants tested, elements such as potassium, sodium, carbon and oxygen were found in the EDS spectrum of implants MT with HSA. As the displacement was greater in the fatigue tests for this sample than for the implants EH and MT with RBM, the artificial saliva was able to enter the foam-implant interstitium, and its inorganic components could be adsorbed onto the rough TiO_2 surface of the implant.

Through the SEM, it was found that the wear tracks in the implants/abutments tested were mainly formed by abrasion, due to the contact of the sample and sphere asperities (figure 3.3). Since CP Ti has less wear resistance than the Ti_6Al_4V alloy [21], it is likely that the loss of mass has been slightly higher for the implants/abutments than for the spheres. Considering that the solids in contact have a similar composition due to the presence of titanium (chemical affinity), it is possible that the delamination has derived from some adhesion of the two surfaces. In addition, there are also indications that the artificial saliva contributed to increase the wear of the samples tested, especially in those that showed higher mean coefficient of friction, to promote the dissolution of the metal [51]. Thus, it is assumed that artificial saliva can also trigger a corrosive action on dental implants even in the absence of fluoride ions, similar to the solutions containing these ions [18, 52].

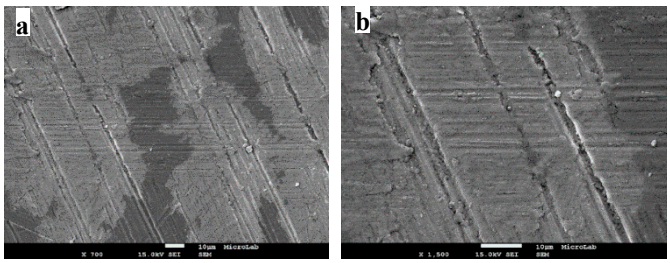

Figure 3.3 – SEM images (700x (**a**) and 1500x (**b**)) of a wear track effected on an abutment MT treated with RBM.

The study of the Ti CP/Ti_6Al_4V tribological pair in artificial saliva performed in this study also appears to be unique because it is not found in the scientific literature. Apparently, the assay of this tribological pair in aqueous environment is different from an assay performed on dry environment [5], showing that saliva is an aggressive environment for metallic dental implants.

4. CONCLUSIONS

Regardless of the type of connection or treatment, dental implant system specimens showed a fatigue behaviour similar to rigid PU foam (elastoplastic), which in turn is identical to that of human trabecular bone. The results demonstrated that increased frequency or mean force promotes a greater displacement of the implants within the PU foam. Also, it can be concluded that the deformation mechanism may be dependent on the type of implant-abutment connection and surface treatment of the implants and the presence of saliva. The connection/treatment MT with HSA showed the greatest deformation, but most of the samples did not reveal the ability to accommodate the micromovements of the implant in the PU structure.

Most of the results of the nanotribological tests indicated that the lubricant was not completely displaced from the space between the sample and the sphere, which means saliva has the ability to penetrate the implant-abutment interface. The cyclic loads in artificial saliva showed little influence on the μ of the tribological pair Ti

CP/Ti_6Al_4V in lubricated environment, but caused more wear on the related-cyclic loading spheres.

The lower BV/TV and Tb.Th values determined in the micro-CT corresponded to the samples with the greatest deformation, like the interface/treatment MT and RBM.

In SEM imagens, the foam related to the MT with RBM and with HSA showed the highest accumulation of damage and the largest affected area by the implant, respectively. The increase in the affected area and/or the number of collapsed cells was related to the increased displacement of the implant. MT interface fixed the abutments to the implants much better than the EH, but the latter allowed better attachment to the artificial foam.

From the EDS spectra, elements present in the saliva were found in the titanium implants MT with HSA, subjected to fatigue tests. So, it is possible to conclude that the inorganic components of artificial saliva adsorb onto the rough TiO_2 surface of the implant.

Besides, the wear tracks in the implants/abutments tested were mainly formed by abrasion, and some adhesion between the two materials may also have been responsible for the delamination. In addition, there are indications that the artificial saliva contributed to increase the wear of the samples tested, promoting the dissolution of the metal [51]. Thus, artificial saliva can trigger a corrosive action on dental implants [18, 52].

5. FUTURE WORK

- Perform the wear rates of the nanotribological tracks using a profilometer. Will there be competition between the rate of spontaneous reconstruction of the oxidative layer and the rate of reaction between the Ti underneath the oxidative layer and the saliva electrolytes?
- Perform tribocorrosion tests to confirm the erosive and corrosive effect of saliva on the implants.
- Replace the PU foams by natural bone in the fatigue tests, in order to approximate the experimental conditions to the *in vivo* conditions.
- Use a liquid cell in the nanotribological tests to avoid the capillary action of the liquid solution, approximating the experimental conditions to those existing in the oral cavity.
- Perform nanotribological tests with and without fatigue tests in dry medium, to then compare these results with those obtained in this work.

REFERENCES

[1] Crespo, R. (2012). “O impacto da falta de dentes (Edentulismo) na qualidade de vida na população e como resolver”. Programa Harvard Medical School Portugal. [Online]. Available: https://hmsportugal.wordpress.com/2012/04/10/o-impacto-da-falta-de-dentes-edentulismo-na-qualidade-de-vida-na-populacao-e-como-resolver/. [Accessed: 14-Out-2016].

[2] Pulec, B. (2012). “In Office Monitoring and Maintenance of Dental Implants”. Dental Implant Life. [Online]. Available: http://www.dentalimplantlife.com/2012/01/in-office-monitoring-and-maintenance-of-dental-implants/. [Accessed: 14-Out-2016].

[3] Nanci, A. (2008). "Ten Cate’s Oral Histology: Development, Structure, and Function", 8th edition. Montreal, Quebec, Canada: Elsevier.

[4] Humphrey, S. *et al*. (2001). “A review of saliva: Normal composition, flow, and function”. Journal of Prosthetic Dentistry, 85. 2, 162–169.

[5] Moreira, V. (2014). “Comportamento tribológico do sistema Zircónia/Ti_6Al_4V utilizado em implantes dentários”. Instituto Superior Técnico.

[6] Anusavice, K. *et al*. (2013). "Phillips Materiais Dentários", 12th edition. Rio de Janeiro, Brazil: Elsevier.

[7] Atsumi, M. *et al*. (2007). “Methods Used to Assess Implant Stability: Surrent status”. International Journal of Oral & Maxillofacial Implants, 22. 743–754.

[8] Oliscovicz, N. *et al*. (2013). “Effect of implant design and bone density in primary stability”. Brazilian Journal of Oral Sciences, 12. 3, 158–163.

[9] Javed, F. *et al*. (2013). "Role of primary stability for successful osseointegration of dental implants: Factors of influence and evaluation". Interventional Medicine & Applied Science, 5. 4, 162–167.

[10] Elias, C. (2011). "Factors Affecting the Success of Dental Implants, Implant Dentistry - A Rapidly Evolving Practice". Instituto Militar de Engenharia, Turkyilmaz, I. Edition. Rio de Janeiro, Brazil: InTech.

[11] Wong, M. *et al*. (1995). "Effect of surface topology on the osseointegration of implant materials in trabecular bone" Journal of Biomedical Materials Research, 29. 1567–1575.

[12] Feitosa, P. *et al*. (2013). "Stability of external and internal implant connections after a fatigue test". European Journal of Dentistry, 7. 3, 267–271.

[13] McArdle, B. (2016). "The Advantages of the Morse Taper Dental Implant Connection," Todays Dental News. [Online]. Available: http://www.dentistrytoday.com/news/todays-dental-news/item/747-the-advantages-of-the-morse-taper-dental-implant-connection. [Accessed: 06-Nov-2016].

[14] Ballo, A. *et al*. (2011). "Dental Implant Surfaces - Physicochemical Properties, Biological Performance, and Trends". Implant Dentistry - A Rapidly Evolving Practice, Turkyilmaz, I. Edition. Rijeka, Croatia: InTech. 1-40.

[15] Elias, C. *et al*. (2008). "Relationship between surface properties (roughness, wettability and morphology) of titanium and dental implant removal torque". Journal of the Mechanical Behavior of Biomedical Materials, 1. 3, 234–242.

[16] Le Guéhennec, L. *et al*. (2007). "Surface treatments of titanium dental implants for rapid osseointegration". Dental Materials, 23. 844–854.

[17] Melo, C. (2015). "Ensaios De Fadiga Mecânica Sobre Conexões Implante - Pilar". University of Fernando Pessoa.

[18] Shemtov-Yona, K. *et al*. (2014). "The effect of oral-like environment on dental implants fatigue performance". Clinical Oral Implants Research, 25. e166–e170.

[19] Shemtov-Yona, K. *et al*. (2014). "Identification of failure mechanisms in retrieved fractured dental implants". Engineering Failure Analysis, 38. 58–65.

[20] Zhou, Z. *et al*. (2008). "Tribology of dental materials: a review". Journal of Physics D: Applied Physics, 41. 1-22.

[21] Zhou, Z. *et al*. (2015). "Biotribology: Recent progresses and future perspectives". Biosurface and Biotribology, 1. 3–24.

[22] Licausi, M. *et al*. (2013). "Tribocorrosion mechanisms of Ti_6Al_4V biomedical alloys in artificial saliva with different pHs". Journal of Physics D: Applied Physics, 46. 1-10.

[23] Sawbones. (2016). "Cranio and Maxillofacial Surgical Catalog". Vashon Island, Washington, U.S.A. 1-14.

[24] Sawbones. (2016). "Biomechanical Test Materials". Vashon Island, Washington, U.S.A. 1-13.

[25] Shim, V. *et al*. (2012). "Use of Polyurethane Foam in Orthopaedic Biomechanical Experimentation and Simulation". InTech. 171–200.

[26] ASTM International. "ASTM F1839 - 08(2016) Standard Specification for Rigid Polyurethane Foam for Use as a Standard Material for Testing Orthopaedic Devices and Instruments". West Conshohocken, Pennsylvania, U.S.A.

[27] DIO Implant. (2013). "DIO Implant Product Catalog (version 3) - SM Torx/ExtraWide Implant System, NarrowFix Implant System, ProTem Implant System, Surgical Instrument, and Dental Product". Yangsan, Kyungnam, South Korea.

[28] DIO Technology Research Institute. "SMile Implant System - Surgical Manual (version 1)". Yangsan, Kyungnam, South Korea. 1-58.

[29] Implant Part. (2017). "RBM SURFACE INFORMATION". [Online]. Available: https://www.implantpart.com/rbm-surface-information/. [Accessed: 26-Fev-2017].

[30] Piattelli, M. *et al*. (2002). "Bone Response to Machined and Resorbable Blat Material Titanium Implants: An Experimental Study in Rabbits". Journal of Oral Implantology, 28. 1, 2–8.

[31] Noris Medical. “RBM Process”. [Online]. Available: https://www.norismedical.com/products/processes/. [Accessed a: 19-Jun-2017].

[32] DIO Implant. (2015). “UFII implant”. 1, Yangsan, Kyungnam, South Korea.

[33] Huang, J. *et al*. (2017). “Nanotubular topography enhances the bioactivity of titanium implants”. Nanomedicine: Nanotechnology, Biology and Medicine. 1–11.

[34] Ayllón, J. *et al*. (2014). “Fatigue Life Estimation in Dental Implants”. Engineering Fracture Mechanics.

[35] Oldani, C. *et al*. (2012). “Titanium as a Biomaterial for Implants”. Recent Advances in Arthroplasty, Fokter, S. Edition. Rijeka, Croatia: InTech. 149–162.

[36] Göhring, T. *et al*. (2004). “In vitro microleakage of adhesive-sealed dentin with lactic acid and saliva exposure: A radio-isotope analysis”. Journal of Dentistry, 32. 235–240.

[37] International Organization for Standardization (ISO). (2007). “ISO 14801:2007(en) Dentistry - Implants - Dynamic fatigue test for endosseous dental implants”. Geneva, Switzerland.

[38] UNI EN ISO. (2006). “Prova di fatica per impianti dentali intraossei”. Milano, Italy. 1-10.

[39] Bicudo, P. (2015). “Comportamento Mecânico de Implantes Dentários”. Instituto Superior Técnico.

[40] Fernandes, P. (2014). “Aplicação da Microtomografia Computadorizada para a Análise Morfométrica Bi e Tridimensional na Avaliação da Perda Óssea Experimental em Ratos”. University of São Paulo.

[41] Scarfe, W. *et al*. (2008). “What is Cone-Beam CT and How Does it Work?”. Dental Clinics of North America, 52. 707–730.

[42] McGarry, J. *et al*. (2008). “Dynamic Evaluation of Forces During Mastication”. Worcester Polytechnic Institute.

[43] Vries, D. (2009). “Characterization of polymeric foams”. Eindhoven University of Technology.

[44] Ashby, M. *et al*. (1983). “The Mechanical Properties of Cellular Solids”. Metallurgical Transactions A, 14A. 1755–1769.

[45] Gibson, L. (2005). “Biomechanics of cellular solids”. Journal of Biomechanics, 38. 377–399.

[46] Gibson L. *et al*, (1999). "Cellular solids: structure & properties", 3rd edition. Cambridge: Cambridge University Press.

[47] Trisi, P. *et al*. (2009). “Implant micromotion is related to peak insertion torque and bone density”. Clinical Oral Implants Research, 20. 467–471.

[48] Pintinha, M. *et al*. (2013). “Effect of mechanical loading on the removal torque of different types of tapered connection abutments for dental implants”. Journal of Prosthetic Dentistry, 110. 5, 383–388.

[49] Jin, Z. *et al*. (2006). “(v) Biotribology”. Current Orthopaedics, 20. 32–40.

[50] Ahmed, E. *et al*. (2014). “The Survival Rate of RBM Surface versus SLA Surface in Geometrically Identical Implant Design”. Journal of Oral Biology, 1. 1, 1–8.

[51] Wennerberg, A. *et al*. (1996). “Experimental study of turned and grit-blasted screw-shaped implants with special emphasis on effects of blasting material and surface topography”. Biomaterials, 17. 15–22.

[52] Licausi, M. *et al*. (2013). “Influence of the fabrication process and fluoride content on the tribocorrosion behaviour of Ti_6Al_4V biomedical alloy in artificial saliva”. Journal of the Mechanical Behavior of Biomedical Materials, 20. 137–148.